

# A combined density functional theoretical and photoelectron spectroscopic study of Ge<sub>2</sub>O<sub>2</sub>

John B. Nicholas and Jiawen Fan

Environmental Molecular Sciences Laboratory, Pacific Northwest Laboratory, MS K2-14, P. O. Box 999, Richland, Washington 99352

Hongbin Wu

Department of Physics, Washington State University, Richland, Washington 99352

Steve D. Colson

Environmental Molecular Sciences Laboratory, Pacific Northwest Laboratory, MS K2-14, P. O. Box 999, Richland, Washington 99352

Lai-Sheng Wang<sup>a)</sup>

Department of Physics, Washington State University, Richland, Washington 99352 and Environmental Molecular Sciences Laboratory, Pacific Northwest Laboratory, MS K2-14, P. O. Box 999, Richland, Washington 99352

(Received 15 February 1995; accepted 21 March 1995)

We study Ge<sub>2</sub>O<sub>2</sub> and Ge<sub>2</sub>O<sub>2</sub><sup>-</sup> with density functional theory (DFT) and photoelectron spectroscopy (PES). We find that Ge<sub>2</sub>O<sub>2</sub> is a rhombus (*D*<sub>2h</sub>), closed-shell molecule with a large HOMO-LUMO gap. The PES spectrum of Ge<sub>2</sub>O<sub>2</sub><sup>-</sup> is obtained at four detachment photon energies: 1064, 532, 355, and 266 nm. Vibrational structure is resolved at the lowest photon energy with a single progression and a frequency of 400 (60) cm<sup>-1</sup>. The experimental adiabatic electron affinity is obtained to be 0.625 (0.050) eV for Ge<sub>2</sub>O<sub>2</sub>. The calculated vertical and adiabatic electron affinities and the HOMO-LUMO gap are in good agreement with the experimental values. The calculated totally symmetric vibrational mode of Ge<sub>2</sub>O<sub>2</sub> (335 cm<sup>-1</sup>) is in reasonable agreement with the observed vibration and represents a Ge-Ge breathing motion. © 1995 American Institute of Physics.

The applicability of using small clusters to model the chemistry of the more complicated bulk materials is a major focus of cluster research. Obtaining a correct description of the structure and bonding of small oxide clusters is an important step in understanding the properties of many environmentally important oxide materials (e.g., minerals and glasses, supported metal oxide catalysis, and zeolites). The best way to accomplish this is to combine both experimental and theoretical approaches. We are mainly interested in silicon oxides,<sup>1</sup> which are ubiquitous in nature. Germanium oxide is also an important material with properties similar to silicon oxide. Thus, information obtained on germanium oxide systems complements our studies of silicon oxides.<sup>1</sup> In this Communication, we present the first quantum calculation and anion photoelectron spectroscopy (PES) study of Ge<sub>2</sub>O<sub>2</sub>. We study both the anion and the neutral molecule, and compare the theoretical and experimental electron affinities and vibrational frequencies.

The Ge<sub>2</sub>O<sub>2</sub> molecule is known to exist in the vapor phase when germanium oxide is thermally vaporized.<sup>2</sup> However, there is little in the literature on Ge<sub>2</sub>O<sub>2</sub>. The only work is by Ogden and Ricks who measured the infrared spectrum of Ge<sub>2</sub>O<sub>2</sub> in a rare gas matrix isolation study and proposed a *D*<sub>2h</sub> ring structure.<sup>3</sup> To our knowledge, there has been no previous theoretical studies of Ge<sub>2</sub>O<sub>2</sub>. In contrast, Si<sub>2</sub>O<sub>2</sub>, which is isoelectronic with Ge<sub>2</sub>O<sub>2</sub>, has been better studied. In an early rare gas matrix infrared experiment, Anderson and Ogden proposed a *D*<sub>2h</sub> ring structure for Si<sub>2</sub>O<sub>2</sub>.<sup>4</sup> Later, Khanna *et al.* studied Si<sub>2</sub>O<sub>2</sub> in a N<sub>2</sub> matrix and assigned their IR and Raman spectra to a bent Si-O=Si-O type of struc-

ture instead.<sup>5</sup> In 1984, Snyder and Raghavachari<sup>6</sup> performed *ab initio* calculations on Si<sub>2</sub>O<sub>2</sub> and concluded that it had a *D*<sub>2h</sub> ring structure, which was also confirmed by a combined matrix/*ab initio* SCF study,<sup>7</sup> a recent mass spectrometric study,<sup>8</sup> and further *ab initio* studies.<sup>8,9</sup>

In the experimental part of this work, we generate the Ge<sub>2</sub>O<sub>2</sub> anion by laser vaporizing a pure germanium target into a helium atmosphere containing 0.05% O<sub>2</sub>. The PES apparatus has been described in detail in previous works.<sup>10-12</sup> Briefly, we employ a magnetic bottle time-of-flight (MTOF) photoelectron analyzer,<sup>13</sup> which has nearly 100% collecting efficiency.<sup>14</sup> A *Q*-switched Nd:YAG vaporization laser (20 mJ output of the second harmonic) is used. The plasma reactions between the laser vaporized germanium atoms and the O<sub>2</sub> seeded in the carrier gas produce a series of Ge<sub>x</sub>O<sub>y</sub><sup>-</sup> clusters. The Ge<sub>2</sub>O<sub>2</sub><sup>-</sup> species has quite low abundance, a likely consequence of the low EA of neutral Ge<sub>2</sub>O<sub>2</sub> (see below). Generation of Si<sub>x</sub>O<sub>y</sub><sup>-</sup> by a similar experimental procedure produces little Si<sub>2</sub>O<sub>2</sub><sup>-</sup>, presumably because Si<sub>2</sub>O<sub>2</sub> is expected to have an even lower EA (our preliminary calculations indicate Si<sub>2</sub>O<sub>2</sub> has a very low EA of ~0.5 eV).

The helium carrier gas and the oxide clusters undergo a supersonic expansion and form a cold molecular beam collimated by two skimmers. The negative clusters are extracted perpendicularly from the beam with a 1 kV high voltage pulse and subjected to a time-of-flight mass analysis. The TOF mass spectrometer has a resolution (*M*/*ΔM*) of about 500 at low masses. The Ge<sub>2</sub>O<sub>2</sub><sup>-</sup> species are mass selected by a three-grid mass gate and subsequently decelerated by a momentum decelerator before interacting with the detach-

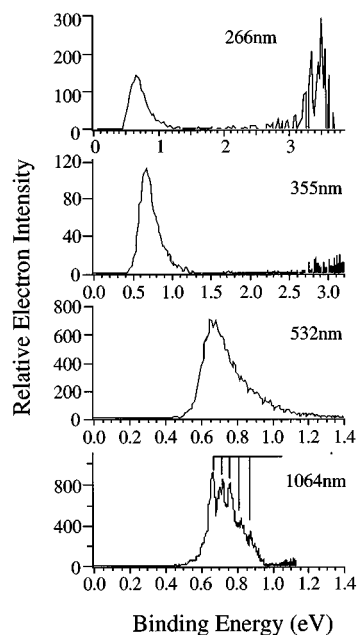


FIG. 1. The photoelectron spectra of  $\text{Ge}_2\text{O}_2^-$  at four different detachment photon energies.

ment laser. Four harmonic outputs (1064, 532, 355, and 266 nm) of another  $Q$ -switched Nd:YAG laser are used for the photodetachment. The electron energies are calibrated with the known spectrum of the  $\text{Cu}^-$  anion and are subtracted from the photon energies to obtain the PES binding energy spectra shown in Fig. 1. The resolution of the TOF spectrometer depends on the electron kinetic energies, giving better resolution for lower energy electrons. The spectrometer has an energy resolution of about 30 meV at 1 eV electron kinetic energy as measured from the spectrum of  $\text{Cu}^-$ . Due to the relatively weak mass signal of  $\text{Ge}_2\text{O}_2^-$ , a rather high laser fluence of  $50 \text{ mJ/cm}^2$  is used for the detachment with 30 000 laser shots at 10 Hz. Three such spectra are taken at the 1064 nm photon energy and summed together to increase the signal-to-noise ratio. The 266 nm spectrum is taken at 20 Hz with the vaporization laser off at alternating shots for background subtraction. Strong noise is present in the 266 nm spectrum for the low electron energy side (beyond 3 eV binding energy). Thus the 266 nm spectrum has poor signal-to-noise ratio at the high binding energy side and is averaged with a 30 meV window.

The 266 nm spectrum shows two features although the feature at high binding energy has quite poor statistics, due to the large spectral noise beyond 3 eV mentioned above. We tentatively assign the second feature to the first excited state of  $\text{Ge}_2\text{O}_2$  which seems to be closed shell with a large HOMO-LUMO gap ( $\sim 2.7 \text{ eV}$ ). It has a rather low electron affinity, as seen in the spectrum, consistent with its relative weak abundance in the cluster beam. To increase the energy resolution, the spectra are also taken at the three lower photon energies, which can only access the ground state of  $\text{Ge}_2\text{O}_2$ . A vibrationally resolved spectrum is observed at 1064 nm with a single progression and a frequency of 400 (60)  $\text{cm}^{-1}$ . The spectrometer transmission of low energy electrons is less efficient and has a cutoff energy near 0.3 eV.

TABLE I. Experimental and theoretical electron affinities and vibrational frequencies for  $\text{Ge}_2\text{O}_2$ .

	Experimental	Theoretical
$\text{EA}_a$ (eV) <sup>a</sup>	0.625(0.050)	0.66
$\text{EA}_v$ (eV) <sup>b</sup>	0.675(0.050)	0.72
HOMO-LUMO gap (eV)	2.7 <sup>c</sup>	2.7 <sup>d</sup>
Vibration ( $\text{cm}^{-1}$ )		
$A_g(1)$		685 <sup>e</sup>
$B_{2u}$	666 <sup>f</sup>	673 <sup>e</sup>
$B_{3u}$	601 <sup>f</sup>	597 <sup>e</sup>
$B_{1g}$		400 <sup>e</sup>
$A_g(2)$	400(60) <sup>g</sup>	335 <sup>e</sup>
$B_{1u}$		69 <sup>e</sup>

<sup>a</sup>Adiabatic electron affinity.

<sup>b</sup>Vertical electron affinity.

<sup>c</sup>Estimate of the energy difference between the second and first features in the 266 nm spectrum in Fig. 1.

<sup>d</sup>The calculated orbital energy between the  $3b_{2g}$  (LUMO) and  $6b_{1u}$  (HOMO) of  $\text{Ge}_2\text{O}_2$ .

<sup>e</sup>Frequencies are scaled by a factor of 1.13 needed to obtain agreement with the literature values for the two IR active  $B_{2u}$  and  $B_{3u}$  modes (see the text).

<sup>f</sup>From Ref. 3.

<sup>g</sup>Current work.

This obviously affects the spectral shape of the 1064 nm spectrum by comparing it with the 532 nm spectrum which is plotted on the same energy scale in Fig. 1. It is clear that the second peak in the 1064 nm spectrum corresponds to the vertical detachment transition. We obtain the adiabatic and vertical EAs of  $\text{Ge}_2\text{O}_2$  as 0.625 (0.050) and 0.675 (0.050) eV, respectively. The large uncertainties are due to a systematic energy calibration error. Relative peak positions can be determined more accurately. The experimental results are summarized in Table I.

To elucidate the structure and bonding of  $\text{Ge}_2\text{O}_2$  and compare with the PES results, we performed theoretical calculations on both  $\text{Ge}_2\text{O}_2^-$  and  $\text{Ge}_2\text{O}_2$  using density functional theory (DFT). We use the DMOL program for the DFT calculations presented here.<sup>15</sup> DMOL employs a form of the DFT that is based on the work of von Barth and Hedin.<sup>16</sup> We use a double zeta polarized basis set, termed DNP in DMOL. A FINE mesh is used to achieve good accuracy in the energy and gradients. We use the local correlation functional of Vosko *et al.*,<sup>17</sup> the gradient-corrected exchange functional of Becke<sup>18</sup> and the gradient-corrected correlation functional of Lee *et al.*<sup>19</sup> The gradient-corrected functionals were used self-consistently. The  $1s$  electrons of O, and the  $1s$ ,  $2s$ , and  $2p$  electrons of Ge, are not included in the molecular orbital expansion or self-consistent procedure. We optimize each molecule with  $D_{2h}$  symmetry using analytical gradients. The optimization is considered converged when the gradient is below 0.001 a.u. and the energy changes by less than  $10^{-6}$  a.u. Diagonalization of the second derivative matrix, obtained from numerical first differences of the analytical gradients, gives the normal mode displacements and frequencies. We calculated the vertical detachment energy (VDE) as the difference in total energy between the optimized geometry of the anion, and the neutral molecule fixed at the anion geometry. The adiabatic detachment energy (ADE) is the difference in total energy between the optimized geometries of the anion and neutral. The calculated vertical and adiabatic

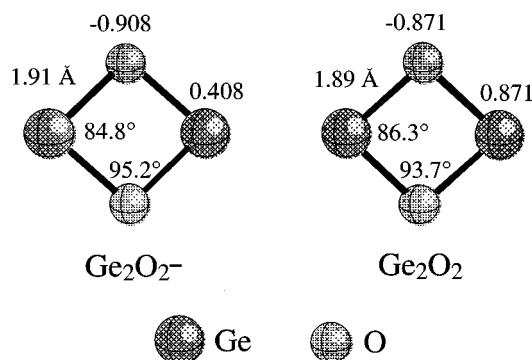


FIG. 2. The DFT optimized  $D_{2h}$  structures of  $\text{Ge}_2\text{O}_2^-$  and  $\text{Ge}_2\text{O}_2$ , showing the bond lengths, bond angles, and the Mulliken charges (in units of  $|e|$ ).

electron detachment energies and vibrational frequencies are compared with the experimental results in Table I.

We show the optimized geometries of both the anion and neutral molecule in Fig. 2, along with the partial charges from a Mulliken population analysis.<sup>20</sup> The lowest energy configurations of both  $\text{Ge}_2\text{O}_2^-$  and  $\text{Ge}_2\text{O}_2$  are  $D_{2h}$ . Most of the difference in geometry between the two molecules involves the Ge-Ge distance, which is 2.75 Å in the neutral, and 2.82 Å in the anion. The O-O distance remains the same in both cases (2.58 Å), while the Ge-O bond length changes by only 0.02 Å. Although care must be taken in interpreting partial charge differences between molecules, the use of the same level of theory and the very small geometry changes between the anion and the neutral, allow some confidence that the partial charge differences are meaningful. The partial charge on O is little changed between the neutral and the anion, while the Ge charge decreases by 0.46  $|e|$ . Thus, the extra electron in the anion is equally split between the two Ge atoms, with negligible additional charge on the O atoms. The fact that the O-O distance is the same in both  $\text{Ge}_2\text{O}_2^-$  and  $\text{Ge}_2\text{O}_2$ , while the Ge-Ge distance increases in the anion, is consistent with the increased repulsion between the two Ge atoms. Theory indicates  $D_{2h}$   $\text{Ge}_2\text{O}_2$  is a closed-shell molecule with a ground state configuration of  $5b_{1u}^2 6a_g^2 3b_{3g}^2 3b_{3u}^2 7a_g^2 2b_{1g}^2 4b_{2u}^2 6b_{1u}^2$ , where the  $6b_{1u}$  HOMO is a bonding orbital. The LUMO ( $3b_{2g}$ ) is a nonbonding Ge  $4p$ -type orbital, in which the extra electron of the anion is localized, in agreement with our interpretation of the partial charges and geometries (Fig. 2).

The closed-shell configuration obtained from the calculations agrees with the observed PES spectra. The first feature in the 266 nm PES spectrum results from removing the extra electrons in the  $3b_{2g}$  orbital of the anion. The second feature, corresponding to removal of a  $6b_{1u}$  electron of the anion, should result in a broader vibrational progression, since the HOMO is a bonding orbital. However, the poor signal-to-noise ratio in this part of the spectrum prevents a thorough characterization of this band. The estimated experimental HOMO-LUMO gap of  $\sim 2.7$  eV is in excellent agreement with the theoretical  $3b_{2g}$ - $6b_{1u}$  orbital energy difference (Table I). The theoretical VDE and ADE are also in good agreement with the experimental results (Table I).

Vibration selection rules predict that the observed vibrational progression should be due to a totally symmetric vi-

bration of the neutral  $\text{Ge}_2\text{O}_2$ . Calculation of the vibrational modes of  $\text{Ge}_2\text{O}_2$  gives two IR active frequencies ( $B_{2u}$ , 596  $\text{cm}^{-1}$  and  $B_{3u}$ , 528  $\text{cm}^{-1}$ ) that agree reasonably well with previous matrix measurements.<sup>3</sup> Scaling these two frequencies to match the experimental values gives an average scale factor of 1.13. The six vibrational frequencies of  $\text{Ge}_2\text{O}_2$ , all scaled by 1.13, are presented in Table I. Two of the vibrational modes are totally symmetric: one  $A_g$  mode, which involves mainly an O-O breathing motion, has a scaled frequency of 685  $\text{cm}^{-1}$ ; the other  $A_g$  mode, which is a Ge-Ge breathing mode, has a scaled frequency of 335  $\text{cm}^{-1}$ . From the calculated changes in partial charge and geometry between the anion and the neutral, we assign the experimentally observed vibration to the 335  $\text{cm}^{-1}$  mode. Although lower frequencies are more difficult to calculate, the predicted frequency is in reasonable agreement with the experimentally measured value.

Finally, it is interesting to compare the similarity between  $\text{Si}_2\text{O}_2$  and  $\text{Ge}_2\text{O}_2$ , which both have the  $D_{2h}$  symmetry. Bulk  $\text{GeO}_2$  and  $\text{SiO}_2$  also have similar structures, with the  $\text{MO}_4$  ( $M=\text{Si, Ge}$ ) tetrahedra being the basic building blocks of both materials. As a structural model, the rhombus  $\text{M}_2\text{O}_2$  clusters can be viewed as part of two edge-shared  $\text{MO}_4$ . Thus it is not surprising that  $\text{Si}_2\text{O}_2$  and  $\text{Ge}_2\text{O}_2$  also have similar structures.

In summary, we found that both  $\text{Ge}_2\text{O}_2^-$  and  $\text{Ge}_2\text{O}_2$  have a  $D_{2h}$  rhombus structure. The extra electron in the anion is added to a nonbonding orbital mostly localized on the two Ge atoms, and does not significantly alter the molecular geometry. The good agreement between theoretical and experimental values of several properties (VDE, ADE, and vibrational frequencies) gives strong support to our interpretation of the geometric and electronic structure of  $\text{Ge}_2\text{O}_2$ . This work illustrates the great utility of an approach that combines both theory and experiment.

## ACKNOWLEDGMENTS

This work is supported by the U. S. Department of Energy, Office of Basic Energy Sciences, Chemical Science Division. Computer resources were provided by the Scientific Computing Staff, Office of Energy Research, at the National Energy Research Supercomputer Center (NERSC), Livermore, California. Pacific Northwest Laboratory is a multiprogram national laboratory operated for the U. S. Department of Energy by Battelle Memorial Institute under Contract No. DE-AC06-76RLO 1830.

<sup>a</sup>To whom correspondence should be forwarded.

<sup>1</sup>J. Fan, J. B. Nicholas, J. M. Price, S. D. Colson, and L. S. Wang, *J. Am. Chem. Soc.* (submitted).

<sup>2</sup>J. Drowart and P. Goldfinger, *Angew. Chem. Int. Ed.* **6**, 581 (1967).

<sup>3</sup>J. S. Ogden and M. J. Ricks, *J. Chem. Phys.* **52**, 352 (1970).

<sup>4</sup>J. S. Anderson and J. S. Ogden, *J. Chem. Phys.* **51**, 4189 (1969).

<sup>5</sup>R. K. Khanna, D. D. Stranz, and B. Donn, *J. Chem. Phys.* **74**, 2108 (1981).

<sup>6</sup>L. C. Snyder and K. Raghavachari, *J. Chem. Phys.* **80**, 5076 (1984).

<sup>7</sup>H. Schnockel, T. Mehner, H. S. Plitt, and S. Schunck, *J. Am. Chem. Soc.* **111**, 4578 (1989).

- <sup>8</sup>N. Goldberg, M. Iraqi, W. Koch, and H. Schwarz, *Chem. Phys. Lett.* **225**, 404 (1994).
- <sup>9</sup>L. Bencivenni, M. Pelino, and F. Ramondo, *J. Mol. Struct.* **253**, 109 (1992).
- <sup>10</sup>J. Fan and L. S. Wang, *J. Phys. Chem.* **98**, 11,814 (1994).
- <sup>11</sup>J. Fan, L. Lou, and L. S. Wang, *J. Chem. Phys.* **102**, 2701 (1995).
- <sup>12</sup>L. S. Wang, H. S. Cheng, and J. Fan, *J. Chem. Phys.* (submitted).
- <sup>13</sup>P. Kruit and F. H. Read, *J. Phys. E* **16**, 313 (1983).
- <sup>14</sup>O. Cheshnovsky, S. H. Yang, C. L. Pettiette, M. J. Craycraft, and R. E. Smalley, *Rev. Sci. Instrum.* **58**, 2131 (1987).
- <sup>15</sup>B. Delley, *J. Chem. Phys.* **92**, 508 (1990).
- <sup>16</sup>U. von Barth and L. Hedin, *J. Phys. C* **5**, 1629 (1972).
- <sup>17</sup>S. J. Vosko, L. Wilk, and M. Nussair, *Can. J. Phys.* **58**, 1200 (1980).
- <sup>18</sup>A. D. Becke, *J. Chem. Phys.* **88**, 2547 (1988).
- <sup>19</sup>C. Lee, W. Yang, and R. G. Parr, *Phys. Rev. B* **37**, 786 (1988).
- <sup>20</sup>R. S. Mulliken, *J. Chem. Phys.* **23**, 1833 (1955).